

## IRIDIUM DISTRIBUTION IN HYDROTHERMALLY SYNTHESIZED Fe, Cu, Zn, AND Pb SULFIDES

SERGEY M. ZHMODIK<sup>§</sup>

*Institute of Geology, Siberian Branch, Russian Academy of Sciences, Koptyuga Avenue, 3, RU-630090 Novosibirsk, Russia*

GENNADY YU. SHVEDENKOV

*Institute of Mineralogy and Petrography, Siberian Branch, Russian Academy of Sciences,  
Koptyuga Avenue, 3, RU-630090 Novosibirsk, Russia*

NATALIA V. VERKHOVTSEVA

*Institute of Geology, Siberian Branch, Russian Academy of Sciences, Koptyuga Avenue, 3, RU-630090 Novosibirsk, Russia*

### ABSTRACT

We have synthesized hydrothermally sulfides of Fe, Cu, Pb, and Zn in the presence of Ir; <sup>192</sup>Ir was employed as the radioactive tracer, and its distribution in run products was determined by autoradiography. None of the synthesized minerals were found to contain Ir in their structure. Instead, there is a characteristic enrichment of Ir along the external surface of individual large crystals or polycrystalline aggregates. Internal parts of sulfide crystals and aggregates lack Ir. We conclude that iridium is concentrated on the surface of growing crystals and polycrystalline aggregates at the crystal–solution interface, and is a result of adsorption equilibrium rather than equilibrium between crystal and solution. As a consequence, coefficients of Ir distribution based on bulk analyses, rather than local analyses of coexisting phases, are not reliable.

*Keywords:* iridium distribution, sulfides, hydrothermal synthesis, iridium, sulfides of Fe, Zn, Pb, Cu, autoradiography.

### SOMMAIRE

Nous avons effectué des synthèses hydrothermales de sulfures de Fe, Cu, Pb, et Zn en présence d'iridium, ajouté sous forme de traceur radioactif <sup>192</sup>Ir, et sa distribution dans les produits de synthèse a été établie par autoradiographie. Aucun des minéraux synthétisés ne semble contenir l'iridium dans leur structure. Par contre, nous voyons un enrichissement caractéristique de l'iridium le long de la surface externe de gros monocristaux ou d'amas polycristallins. Les parties internes des cristaux ou d'aggrégats ne montrent pas d'iridium. A notre avis, l'iridium est concentré à la surface des cristaux et des amas polycristallins à l'interface cristal–solution, et résulte d'un équilibre d'adsorption plutôt que d'un équilibre entre cristal et solution. Par conséquent, les coefficients de distribution de l'iridium déduits à partir de compositions globales, plutôt que de compositions locales des phases coexistantes, ne seraient pas fiables.

(Traduit par la Rédaction)

*Mots-clés:* distribution de l'iridium, sulfures, synthèses hydrothermales, iridium, sulfures de Fe, Zn, Pb, Cu, autoradiographie.

---

<sup>§</sup> *E-mail addresses:* zhmodik@uiggm.nsc.ru, vnathali@uiggm.nsc.ru

## INTRODUCTION

In recent years, a large body of data has appeared regarding the high concentration of platinum-group elements (PGE) in low-temperature formations related to hydrothermal and sedimentary processes. Ore-grade concentrations of the PGE have been found in rocks and ores of hydrothermal gold deposits, black shale, ocean-floor hydrothermal ores, and ferromanganese nodules; furthermore, a high mobility of the PGE during the development of weathered crusts was also established (Baturin 1993, Rudashevskii *et al.* 1995, Shor *et al.* 1996, Laverov *et al.* 1997, 2000, Korobeinikov *et al.* 1998, Anikeeva *et al.* 1999, Ermolaev *et al.* 1999, Kucha & Przybylowicz 1999, Peucker-Ehrenbrink & Hannigan 2000). In many cases, the concentrations of the PGE in ores and rocks are confined to sulfide minerals, but the mode of occurrence of these elements commonly is not established. In ores of the aforementioned types of deposit, iridium is invariably present in platinum-group minerals and, therefore, can be chosen as a good monitor of the geochemical behavior of PGE.

## EXPERIMENTAL METHOD

Sulfides of Fe, Cu, Pb and Zn were synthesized hydrothermally in the presence of  $^{192}\text{Ir}$ , which was used as a tracer and analyzed for by radiography (Mironov *et al.* 1989). Experiments were carried out at 500 bars in a steel autoclave with a titanium insert. The volume, main-

tained at  $55\text{ cm}^3$ , was preset according to the P-T-X diagram for aqueous  $\text{NH}_4\text{Cl}$  solutions. Experiments were run at  $400^\circ$  and  $500^\circ\text{C} \pm 3^\circ\text{C}$ . A temperature gradient of  $14^\circ\text{C}$  was maintained between the upper and lower zones of the pressure vessel. The run duration ranged from 100 to 1000 h. Three experimental systems, Fe-Pb, Fe-Cu, and Fe-Zn, were investigated with the aim of synthesizing sulfide minerals. Each 10 g charge was prepared from elements of high-purity grade in stoichiometric proportions for pyrite, galena, chalcopyrite, and sphalerite. The recrystallizing solution was 2.06 M ammonium chloride. Eleven to 74 ppm of Ir was added to the charge in the form of a hydrochloric acid solution of  $\text{Na}_2[\text{IrCl}_6]$  at a pH of 3.5.

The radioisotope  $^{192}\text{Ir}$  was produced by the reaction  $^{190}\text{Ir} (n, \gamma) \rightarrow ^{192}\text{Ir}$  in a nuclear reactor at the Research Institute of Nuclear Physics of the Tomsk Polytechnic University (Fig. 1). The water-soluble compound of iridium was obtained by chlorination of metallic Ir (99.9% pure), which had previously been doped with the irradiated Ir. The doped Ir metal was placed in a silica tube in the middle of the furnace area, together with NaCl powder. The temperature in the central part of the reaction tube was  $950^\circ\text{C}$ . Although there are large temperature-gradients at the ends of the furnace, more than  $200^\circ\text{C}$  over 1 cm, the temperature in the central part was stable in the range  $900\text{--}950^\circ\text{C}$  over 11 cm. The duration of chlorination was 2.5 hours at a rate of about  $3\text{ dm}^3$  of  $\text{Cl}_2$  per hour. In as little as 0.5 hours, the displacement of the zone of maximum activity from the center of the

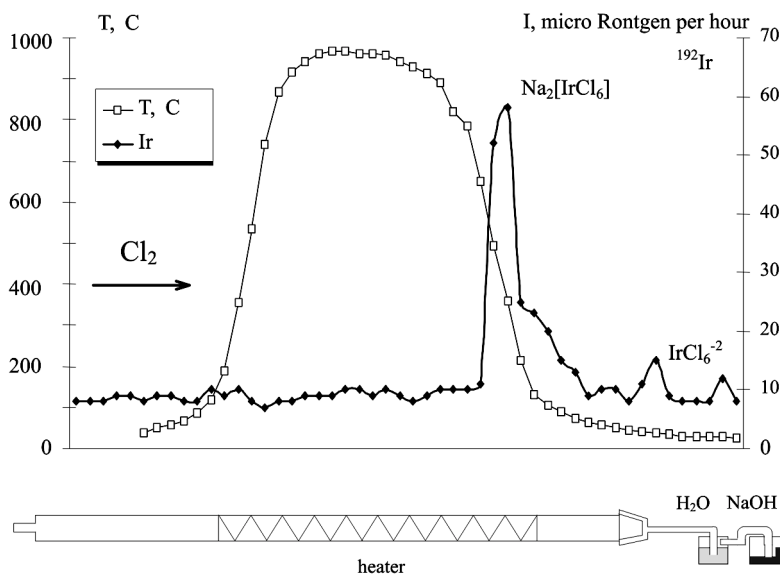


FIG. 1. Schematic representation of experimental results of Ir gaseous transfer of iridium in a  $\text{Cl}_2$  stream.

furnace in the direction of the chlorine flow was fixed. After 1 hour, most of the iridium was concentrated at the end of reaction tube. After 2–2.5 hours of chlorination, 80–90% of the metal was concentrated with a minimal difference in temperature at the end of the reaction tube. At the upper part of the silica tube, a thin brownish red coating was formed, which was easily washed off with a HCl solution (pH = 3.5). Most of the Ir precipitated in the portion of the tube that was below 480°C, and none was observed beyond the point where temperatures exceed 600°C. A small amount of Ir, constituting less than 5% of the amount originally added to the tube, did not dissolve but remained on wall of the silica tube.

The radioisotope  $^{192}\text{Ir}$  is a beta-emitter with a half-life period of 74.4 days, making it suitable for establishment of the spatial distribution and the forms of iridium occurrence in the minerals synthesized by means of beta-autoradiography. Beta-emission was detected using MP-type emulsion for nuclear studies and AF-type film for autoradiography.

The following crystals and polycrystalline aggregates were synthesized: pyrite, pyrrhotite, and galena (Fe–Pb system), pyrite, chalcopyrite, bornite, chalcocite, and pyrrhotite (Fe–Cu system), pyrite, pyrrhotite, ferroan sphalerite, and sphalerite (Fe–Zn system). Frag-

ments of mineral aggregates and crystals were embedded with epoxy resin and polished with diamond paste for autoradiographic and mineragraphic studies. At the end of an experiment, we measured the  $\gamma$ -activity of the solution (with the use of standards), the sulfides synthesized, and the titanium inserts.

## RESULTS

At the end of the experiments, all of the iridium introduced into the experimental systems was found to be closely associated spatially with the synthesized sulfides. There was no Ir in the solutions nor on the titanium inserts. Figure 2 shows polished fragments of aggregates of synthetic sulfides and crystals,  $\beta$ -autoradiograms registering the distribution of Ir, and profiles of Ir concentration. The characteristic feature of the spatial distribution of Ir is its enrichment on external surfaces of individual large crystals or polycrystalline aggregates. Internal parts of sulfide crystals and aggregates lack Ir. This distribution is characteristic of all of the sulfide minerals, pyrite, chalcopyrite, bornite, pyrrhotite, galena, and sphalerite. No separate mineral of iridium was revealed by autoradiography data and by scanning electron microscopy. In rare cases, dispersed concentrations of Ir were noted included within the

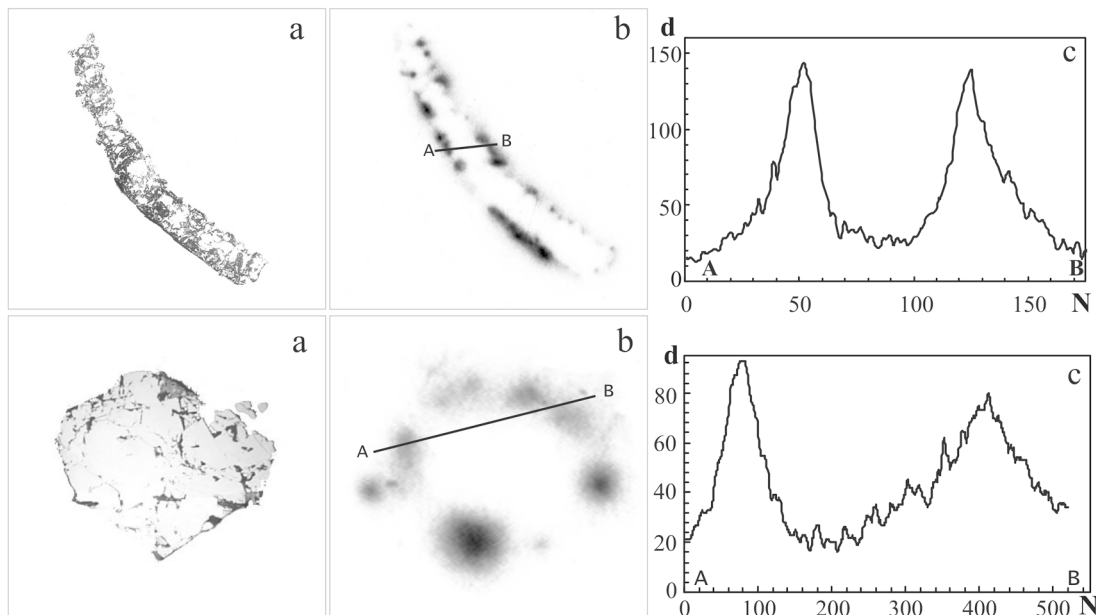


FIG. 2. Photomicrographs of (a) sulfides of chalcopyrite and sphalerite, (b)  $\beta$ -radiograms showing Ir distribution (based on  $^{192}\text{Ir}$ ), and (c) relative concentrations of Ir in profiles, expressed by color density (d, relative units). Maximal density of autoradiograms corresponds to maximal Ir concentration. The upper row is for chalcopyrite; the lower row, sphalerite. Exposure time is 10 h. Nuclear emulsion is of the AF type. The abscissa shows the number of points in a profile (point size is 10.6  $\mu\text{m}$ ; dimension of the AB section in the upper row is 1.7 mm).

sulfide minerals, but they could not be analyzed owing to their exceedingly small size.

The level of concentration of Ir on sulfide surfaces decreases toward the final stages of the experiments as the aqueous  $\text{NH}_4\text{Cl}$  solution becomes depleted in Ir. In many cases, the last-formed sulfide crystals lack iridium.

None of the minerals synthesized appears to contain Ir in solid solution. Iridium is concentrated only at the surface of the growing crystals and polycrystalline aggregates, *i.e.*, at the crystal–solution interface. The distribution of Ir between sulfides and solution therefore appears to result from an adsorption equilibrium. In order to assess the distribution of Ir into the sulfide from the sulfide–solution boundary, profiles were determined (Fig. 3). The curves showing intensity of  $\beta$ -tracks at the sulfide–solution boundary (Fig. 3a) are asymmetrical and characterized by a gradual increase in the Ir concentration from solution to the sulfide surface, *i.e.*, they are more flattened than those at the boundary between the sulfide surface and the subsurface part of a crystal (Fig. 3b, Section 2). Curves fitted to the data describe the Ir concentration in the crystal surface–solution section (Fig. 3a) and the crystal surface – subsurface section (Fig. 3b). The variation in Ir concentration in Section 1 is described by the following equation, and has a squared cross-correlation ( $R^2$ ) of 0.966:

$$y = y_0 + A_1 e^{-x/t_1} + A_2 e^{-x/t_2} \quad (1),$$

where  $y$  is iridium concentration,  $y_0$  is iridium concentration at time zero,  $A_1$  and  $A_2$  are constants, and  $t_1$  and  $t_2$  are time intervals.

According to Hall's hypothesis (Kröger 1964, Hall 1953, Chernov 1960), the distribution coefficient depends on growth rate and is described by the following expression, which entirely characterizes the tracer dis-

tribution in the growing crystal in the case of adsorption equilibrium:

$$k_{\text{eff}} = k + (k_{\text{ads}} - k)e^{-v_{\text{sl}}/v} \quad (2),$$

where  $v$  is the growth rate,  $v_{\text{sl}}$  is the rate of transfer of a tracer atom between crystal and adjacent solid and aqueous phase,  $k_{\text{ads}}$  is the coefficient of adsorption, and  $k$  is the coefficient distribution ( $k_{\text{eff}} = k$  if  $v_{\text{sl}} > v$ , and  $k_{\text{eff}} = k_{\text{ads}}$  if  $v > v_{\text{sl}}$ ). The dependence of  $k_{\text{eff}}$  on the growth rate is explained by formation of an adsorbed layer at the phase boundary.

Equations (1) and (2) are correlated. Therefore, according to Hall's hypothesis (Kröger 1964, Hall 1953), tracer atoms (in this case, Ir) are initially adsorbed on the interface, and only subsequently do they enter into the crystal structure. At a low growth-rate, the adsorbed layer moves in front of the interface and is sustained owing the fast exhumation of atoms of the solid phase, which were originally adsorbed and captured by the growing crystal. This inference is corroborated by analysis of the curve in Section 2, corresponding to the boundary between the crystal surface and the subsurface region of crystal (Fig. 3b). Here, the concentration of Ir is described by a sigmoidal curve, consistent with Hall's hypothesis and the distribution of the tracer in solid-phase reactions (Tret'yakov 1978).

An alternative explanation for the observed  $\beta$ -track patterns is that all of the Ir is hosted by numerous very small crystals of an Ir-bearing phase deposited during the quench of the experiments directly on the surface of the sulfide minerals. These would act as point sources of  $^{192}\text{Ir}$   $\beta$ -tracks located exactly on the surface, and the widths and shapes of the profiles could simply represent the statistical distribution of travel distances of  $\beta$ -particles emitted from these point sources. In this case, the observed pattern of iridium distribution could result

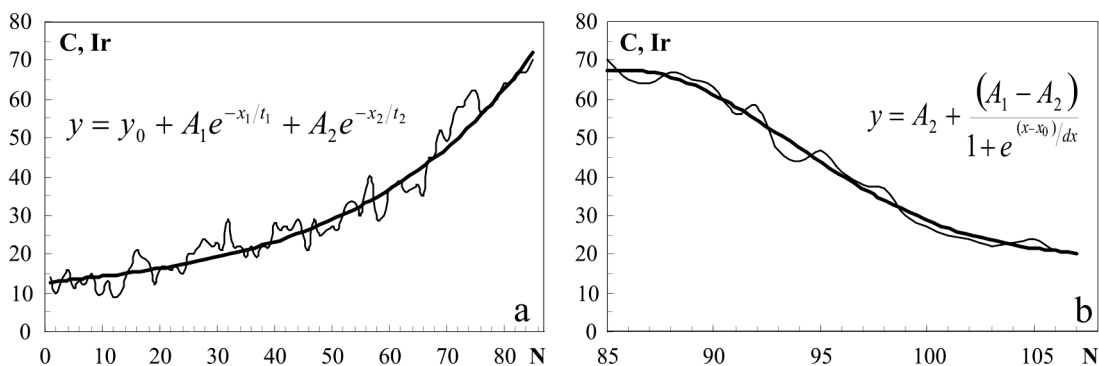


FIG. 3. Variations in Ir concentration ( $C_{\text{Ir}} = d$ ) in synthesized sulfides. (a) The external surface of sulfides (adjacent to the solution) – boundary zone; (b) boundary zone – subsurface part of the sulfides. N: number of points (length of profiles: a: 935  $\mu\text{m}$ , b: 242  $\mu\text{m}$ ).

from deposition of iridium from aqueous solution only at the time of quenching of the experimental charge. We do not accept this explanation for the following reasons: 1) In several cases, we have observed Ir enrichment along grain boundaries within polycrystalline aggregates of sulfides (sphalerite, pyrite). These grain boundaries were isolated from the solution at the end of the experiment, making it unlikely that Ir could have migrated into such confined spaces during the quench. The distribution of iridium in such crystals is of the same type as we described, *i.e.*, Ir is concentrated in the surface part of crystals. 2) Profiles of  $\beta$ -tracks across the mineral surfaces are asymmetrical, being better fitted by exponential curves outside the crystals but by sigmoidal curves within the sulfide crystals. Whereas the exponential curves outside the crystals could be interpreted as resulting from the random dispersal of  $\beta$ -particles through the epoxy mounting medium (exponential decay away from the source), the sigmoidal patterns within the sulfides are better accounted for as being truly representative of concentration profiles within the minerals. If all of the iridium were to be concentrated in a thin surface-layer, we would expect to see exponential profiles on both sides, with different distances of penetration as a result of the different mean free path in the sulfide and epoxy media.

#### DISCUSSION

Experiments on the hydrothermal synthesis of Ir-bearing sulfides have established that Ir is not incorporated in the structure of the sulfides of Fe, Cu, Pb, and Zn at concentrations detectable by autoradiography. The distribution of iridium between solution and sulfide corresponds to an adsorption equilibrium rather than equilibrium between crystals and aqueous solutions. The growth rate of crystals was low (between  $3 \times 10^{-6}$  and  $3 \times 10^{-9}$  cm/s) in the experiments. At very high rates of crystal growth, Ir concentrations in sulfide minerals may be sufficiently evenly distributed within the mineral volume, owing to the fast overgrowth of the newly formed adsorption layer by the mineral-forming elements of growing crystal. In a closed system, this process could lead to the development of zoned Ir concentrations. Apparently, in the Fe, Cu, Pb, Zn sulfides synthesized hydrothermally from a solution, the coefficient of Ir distribution ( $C_s/C_l$ ) is less than 1. In this case, the distribution is controlled by adsorption and results in an "effective coefficient of distribution" rather than a true coefficient of distribution, in which the element is incorporated in the structure. As a consequence of these results, coefficients of Ir distribution based on results of bulk analyses, rather than on results of local micro-analyses of coexisting phases, may be inconsistent with true values.

#### ACKNOWLEDGEMENTS

This work was supported by the Russian Foundation for Basic Research, project no. 00-05-65332. The authors greatly appreciate constructive reviews of the article by referees S.D. Scott and A. Peregoedova. We are very grateful to J.E. Mungall for his remarks, which helped us to improve our article.

#### REFERENCES

- ANIKEEVA, L.I., ANDREEV, S.I., ALEKSANDROV, P.A., ZADORNOV, M.M., NOVIKOV A.B., KAZAKOVA V.E. & KUROCHKINA, A.M. (1999): Platinum-bearing Fe–Mn formations of the world's oceans. *In* Platinum of Russia: Problems of the Development of Raw Mineral Base for Platinum Metals in the 21st Century. Geoinformark, Moscow, Russia (338-345; in Russ.).
- BATURIN, G.N. (1993): *Ores of the Ocean*. Nauka, Moscow, Russia (in Russ.).
- CHERNOV, A.A. (1960): On the theory of unbalanced capture of admixtures during crystal growth. *Dokl. Akad. Nauk SSSR* **132**(4), 818-821 (in Russ.).
- ERMOLAEV, N.P., SOZINOV, N.A., CHINENOV, V.A., GORYACHKIN, N.I. & KHOROSHILOV, V.L. (1999): Metal-bearing black schists – new perspective source of platinum metals. *In* Platinum of Russia: Problems of the Development of Raw Mineral Base for Platinum Metals in the 21st Century. Geoinformark, Moscow, Russia (212-226; in Russ.).
- HALL, R.N. (1953): Segregation of impurities during the growth of germanium silicon crystals. *J. Phys. Chem.* **57**, 836-838.
- KOROBENIKOV, A.F., MITROFANOV, G.L., NEMEROV, V.K. & KOLPAKOVA, N.A. (1998): Untraditional gold–platinum deposits of eastern Siberia. *Geol. Geofiz.* **4**, 426-438 (in Russ.).
- KRÖGER, F.A. (1964): *The Chemistry of Imperfect Crystals*. North-Holland Publ. Co., Interscience Publishers, Amsterdam, The Netherlands.
- KUCHA, H. & PRZYBYLOWICZ, W. (1999): Noble metals in organic matter and clay-organic matrices, Kupferchiefer, Poland. *Econ. Geol.* **94**, 1137-1162.
- LAVEROV, N.P., DISTLER, V.V., MITROFANOV, G.L., NEMEROV, V.K., KOVALENKER, V.A., MOKHOV, A.V., SEMEIKINA, L.K. & YUDOVSKAYA, M.A. (1997): Platinum and other native metals in ores of Sukhoj Log gold deposits. *Dokl. Ross. Acad. Sci.* **355**, 904-907.
- \_\_\_\_\_, LISHNEVSKII, E.N., DISTLER, V.V. & CHERNOV, A.A. (2000): Model of the ore-magmatic system of the Sukhoj Log gold–platinum deposit, eastern Siberia, Russia. *Dokl. Ross. Akad. Nauk* **375**, 1362-1365 (in Russ.).

- MIRONOV, A.G., AL'MUKHAMEDOV, A.I., GELETYI, V.F., GLUCK, D.S., ZHATNUEV, N.S., ZHMODIK, S.M., KONNIKOV, E.G., MEDVEDEV, A.YA. & PLYUSNIN, A.M. (1989): *Experimental Studies of the Geochemistry of Gold with the Help of Radioisotope Indicators*. Nauka, Novosibirsk, Russia.
- PEUCKER-EHRENBRINK, B. & HANNIGAN, R.E. (2000): Effects of black shale weathering on the mobility of rhenium and platinum group elements. *Geology* **28**, 475-478.
- RUDASHEVSKII, N.S., KNAUF, V.V. & CHERNYSHOV, N.M. (1995): Platinum-group minerals from black shales KMA. *Dokl. Ross. Akad. Nauk* **344**, 91-95 (in Russ.).
- SHOR, G.M., DITMAR, G.V., KOMAROVA, N.I. & GOLIKOVA, O.V. (1996): Formation of the infiltration-type mineralization of platinum group elements in the West Siberian platform cover. *Dokl. Ross. Akad. Nauk* **351**, 525-527 (in Russ.).
- TRET'YAKOV, YU.D. (1978): *Solid-Phase Reactions*. Nauka, Moscow, Russia (in Russ.).
- Received May 31, 2003, revised manuscript accepted March 19, 2004.*